J Mater Sci: Mater Med (2006) 17: 387–396
DOI 10.1007/s10856-006-8243-9

Organic-inorganic interaction and the growth mechanism of hydroxyapatite crystals in gelatin matrices between 37 and 80 °C

Myung Chul Chang · William H. Douglas · Junzo Tanaka

Received: 23 October 2003 / Accepted: 6 May 2005

Abstract The crystal development of hydroxyapatite[HAp] phase in gelatin[GEL] matrices was investigated in the temperature range 37 to 80 °C by using X-ray diffraction, scanning electron microscopy(SEM), thermoanalytical measurement(DT/TGA), Fourier-Transformed Infra-Red(FT-IR) spectroscopy, and transmission electron microscopy(TEM) with electron diffraction(ED). It was found that during the coprecipitation of apatite phase in GEL matrices and the next aging process the crystallites were formed and developed through the two reaction mechanisms of organic-inorganic interaction between apatite phase and GEL molecules, and thermodynamic reaction for the crystal growing. The analytical evidences showed that there was a definite competition between these two mechanisms with the reaction temperature. Below 50 °C the crystal development of HAp was greatly suppressed by the existence of the GEL molecules, indicating the heterogeneous nucleation by the supposed number of carboxyl groups in GEL. Above 50 °C the effective organic components as a template for the heterogeneous nucleation of apatite crystallites were greatly degraded and so more amount of inorganic ions could be favorably accredited on the preexisting crystallites in virtue of the limited nucleation chance, finally resulting in the crystal growth. At higher temperature pretty big HAp crystals were developed with the depletion of the organics to be bound with crystallites in the slurry solution. Presumably it is believed that the poisoning of the functional groups in GEL molecules was vigorously occurred in the phosphoric acid environment above ∼50 °C.

M. C. Chang (✉)
School of Mat. Sci. and Chem. Eng., Kunsan National University, Kunsan 573-701, Korea
Tel. : +82-63-469-4735;
Fax: +82-63-466-2086
e-mail: mcchang@kunsan.ac.kr (M C Chang)

J. Tanaka
Biomaterials Center, NIMS, Ibaraki 305-0044, Japan

M. C. Chang · J. Tanaka
CREST, Japan Science and Technology corporation

M. C. Chang · W. H. Douglas
MDRCBB, Dept. of Oral Science, School of Dentistry, University of Minnesota

1. Introduction

In general HAp is a main component of bone mineral and in some cases carbonate-apatite is a main hard tissue component, as in dental enamel. Calcified tissue, such as bone and teeth is basically considered a biologically and chemically bonded composite between HAp nanocrystals and type-I collagen [1, 2]. Researchers have tried to develop the synthetic bone using the biomimetic process [3–7], which is based on the idea that biologic systems store and process information at the molecular level. For decades double diffusion process [8–11] has been widely used in order to study the *in vitro* formation of biologic apatite phase in a stationary system. From several years ago HAp/COL nanocomoposite has been developed through the coprecipitation reaction of HAp nanocrystals in the soluble collagen [12–16]. The characteristic feature of this process is the dynamic reaction using active $Ca(OH)_2$ precursor [12] as a free Ca^{2+} source instead of $CaCl_2$ or $Ca(NO_3)_2$. Recently we have focused on the development of HAp/GEL nanocomposite [17, 18] using the commercial sources of GEL materials. GEL materials have been well studied over several decades [19, 20], but most of research has been focused on the physico-chemical properties of GEL itself. The information about the chemical reaction between GEL and calcium phosphate minerals has been

less known [10, 11, 17, 18] even though a large part of commercial GEL is produced from the calcified hard tissue such as cow bone.

The development of apatite phase in GEL matrices is very complicate [17, 18] because the commercial GEL contains variety of protein species and the different stages of degraded products. Until now our accumulated experimental results have showed that a single morphology of apatite phase could be obtained through the highly vigorous stirring during the coprecipitation or the introduction of fluoride source. In the development of HAp/GEL nanocomposite most of interests are related with the formation of apatite crystals in the GEL matrix and the chemical coordination between the formed apatite crystals and the matrix GEL. The revealing of the strength in the compact body of HAp/GEL composite will be governed by the chemical coordination of HAp crystals with GEL matrices and the directional development of needle-type HAp particles. The biomineralization of GEL matrices by apatite phase was investigated with the preparation temperature on a basis of the organic-inorganic bond formation and the crystal development of apatite phase.

2. Materials and methods

The preparation details of HAp/GEL nanocomposite were well described by Chang [17]. The precursors used here were $CaCO_3$ (Alkaline analysis grade, Wako, Japan), H_3PO_4 (AP grade, Wako, Japan), Gelatin (Nitta Gelatin, Osaka, Japan). $Ca(OH)_2$ powders were obtained through the calcination of $CaCO_3$ powders and the slaking process. The amount of $Ca(OH)_2$ and H_3PO_4 was calculated to make 10g of HAp. The amount of GEL was mostly set as 1g and in some cases we prepared 3–5g GEL batches. Before the coprecipitation the $Ca(OH)_2$ powders were vigorously stirred in DI water at room temperature for 12 hrs and the weighed GEL powders were dissolved in the mixture solution of DI water and phosphoric acid at 37 °C for 12 hrs to help the homogenization of less denatured GEL coils such as worm–like chains [18]. During the entire coprecipitation process we applied the vigorous stirring and the pH was controlled as 8.0 using the digital pH controller. The reaction temperature was changed as 37 °C, 47°C, 50°C, 65°C and 80°C, respectively. The sample names are coded as HG1-47, HG1-65, HG1-80, HG2-47, HG3-50 and HG4-37, respectively. HG1-47 and HG3-50 denote a HAp 10g/GEL 1g sample prepared at 47 °C and a HAp 10g/GEL 3g sample prepared at 50 °C, respectively. After the reaction, the obtained slurry in the solution was aged at the reaction temperature for 24h. A part of slurry was collected after aging and microstructures were characterized by transmission electron microscopy TEM (JEM-1210, JEOL, Japan). The filtered cakes were dried at 37 °C in the incubator and phase formation was confirmed using X-Ray Diffraction (AFC-5R, Rigaku, Japan) on the crushed powders. For the dry body microstructures were characterized using scanning electron microscopy (SEM, JSM-5600, JEOL, Japan). A chemical interaction between HAp crystals and functional groups of GEL was estimated using the diffuse reflectance FT-IR (Spectrum 2000, Perkin-Elmer, UK). Following initial analysis of the raw spectra to determine the precise constituents, the spectral band positions were analyzed by using GRAMS AI(7.0) (Thermo Galactic, Salem, USA).

Thermal analysis (TG-DTA TG8120, Rigaku, Japan) was carried out on the dried samples to evaluate GEL content. The measurements were done between 25 °C and 1200 °C at a heating rate of 10°C/min. All experiments were carried out in Platinum pans in air atmosphere, and Al_2O_3 powders (10mg) were used as a reference. Three-point bending strength and Young's modulus were measured by a universal testing machine(AGS-H, Shimadzu, Japan) at a cross-head of 500 μm /min with a span of 15mm and the typical samples size was $5 \times 3 \times 20 mm^3$.

3. Results and discussion

3.1. XRD analysis

From XRD diffraction pattern (Fig.1) HAp was identified as a main phase for all samples. Most of peaks in HG1-65 and HG1-80 samples were distinctly observed, but the other samples prepared at 37–47 °C showed the broad weak peaks. The input amount of GEL precursor for the constant amount of HAp (10 g) affects the crystal development of HAp in GEL matrix [17]. In a reaction batch the amount of GEL molecules can be considered to be equal to the total number of functional group ($RCOO^-$) to nucleate the HAp crystals on the GEL molecule [2, 17]. With the increase of GEL quantity the size of the developed crystals is reduced and so HAP-37 shows relatively stronger XRD peaks compared to those of HG4-37 and HG2-47. It is noted that the crystal development in HG2-47 batch was quite suppressed through the supply of more amount of GEL, in spite of its higher reaction temperature. On the other hands we could confirm a kind of strong peaks development in HG3-50 sample as shown in HG1-65 and HG1-80. We can say that the crystal growing behavior of HAp phase in GEL matrix is critically transited at the around of 50°C and this transition is supposed to be attributed to the critical degradation of GEL precursor.

The XRD results (inner diagram of Fig. 1) show that the higher amount of organic coordination in the HAp/GEL composite induced the contraction in the (002) lattice dimension. It is known that the lattice parameters of synthetic and biological apatites are influenced by the incorporation of CO_3 for OH^- site and/or PO_4^{3-} site in HAp [21]. The substitution of OH^- in HAp by CO_3^{2-} induces the expansion in the

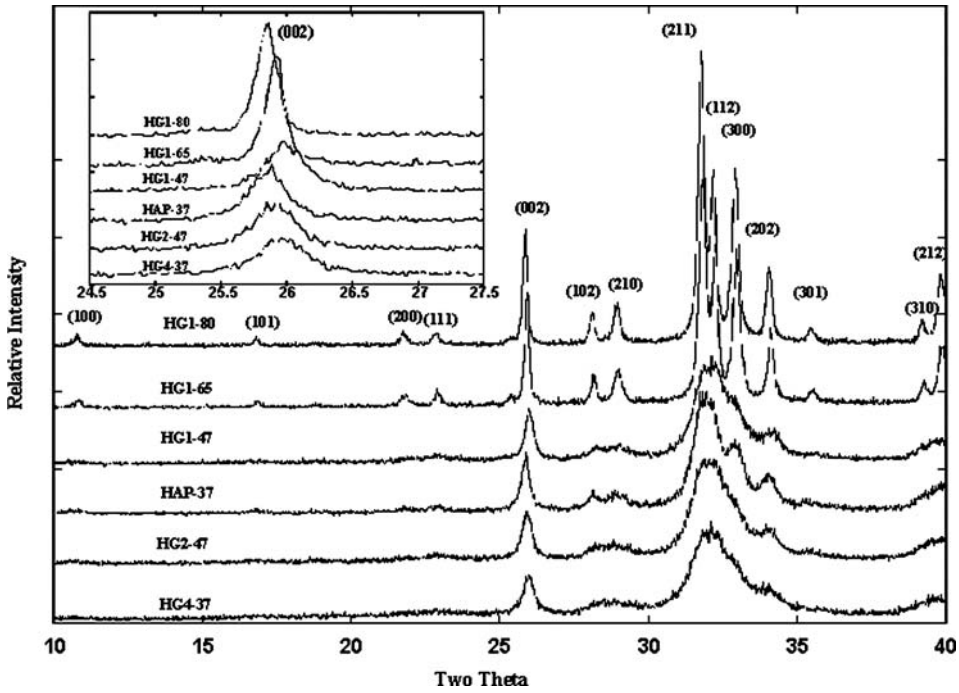

Fig. 1 XRD diffraction pattern for HAp and HAp/GEL composite samples (HG1-47, HG1-65, HG1-80, HAp-37, HG2-47, HG4-37) prepared between 37−80°C. Inner diagram shows the variation of (002) lattice.

a-axis dimension and the contraction in the c-axis dimension, and the substitution of PO_4^{3-} in HAp by CO_3^{2-} induces the contraction in the a-axis dimension and the expansion in the c-axis dimension [21]. From FT-IR spectra (Fig. 3C) HG1-47 sample is supposed to be less carbonated, but HG1-65 and HG1-80 is highly carbonated as like as HAP-37. The CO_3^{2-} substitution in this coprecipitation reaction is mostly B-type(PO_4^{3-}) for all HAp/GEL samples. The (002) lattice contraction in less mineralized samples (Fig. 1) shows that it is hard to simply discuss the lattice change using CO_3^{2-} substitution for HAp. One of possible explanations is that the (002) lattice contraction in the less mineralized sample may be due to the interfacial structure between GEL matrices and the tiny HAp crystallites.

3.2. DT/TG analysis

From DT data (Fig. 2) all HAp/GEL composite samples show strong exothermic peaks at 320°C (T1) and HG1-47 shows another exothermic shoulder at 435°C (T2). T1 corresponds to the thermal degradation and pyrolyzation of GEL molecules, and T2 is associated with the final thermal degradation of the residual organics. From TG data the content of organics in HG1-80 is evaluated as ∼ 60 wt% of that in HG1-47. The TG curve feature between 250 °C and 400 °C shows a very close pattern between HG1-65 and HG1-80 samples, but in HG1-47 the weight loss is rapidly decreased. The estimated amount of organic component in HG1-65 and HG1-80 was greatly reduced in comparison with HG1-47.

Endothermic peak by the hydrated water is appeared below 100°C. The estimated dehydration temperatures for HG1-47 and HG1-80 are 75°C and 60°C, respectively. In HG1-60 and HG1-80 the H_2O molecules are more weakly bound to HAp crystal surface. The water component is partially associated with the organic component and the individual apatitic crystals. Another endothermic temperature was located at just below 800°C for HG1-47, corresponding to the release of carbon dioxide from carbonated apatite. It is interesting that the endothermic peaks by the CO_2 releasing moved to the higher temperature of ∼970°C and ∼1030°C for HG1-65 and HG1-80, respectively. The present experimental results show that the high temperature reaction greatly helps the stable incorporation of CO_3^{2-} into HAp lattice.

3.3. FT-IR spectra

3.3.1. Chemical bond formation

Amide I and amide II band

FT-IR data (Fig. 3A) tell us more information about organic-inorganic interaction between HAp phase and GEL matrices. HG1-47 shows the strong amide bands; amide I in the range 1700–1600 cm^{-1} and amide II in the range 1600–1460 cm^{-1}. On the other hands HG1-65 and HG1-80 show the weak amide II band, indicating the decrease of organic coordination of HAp.

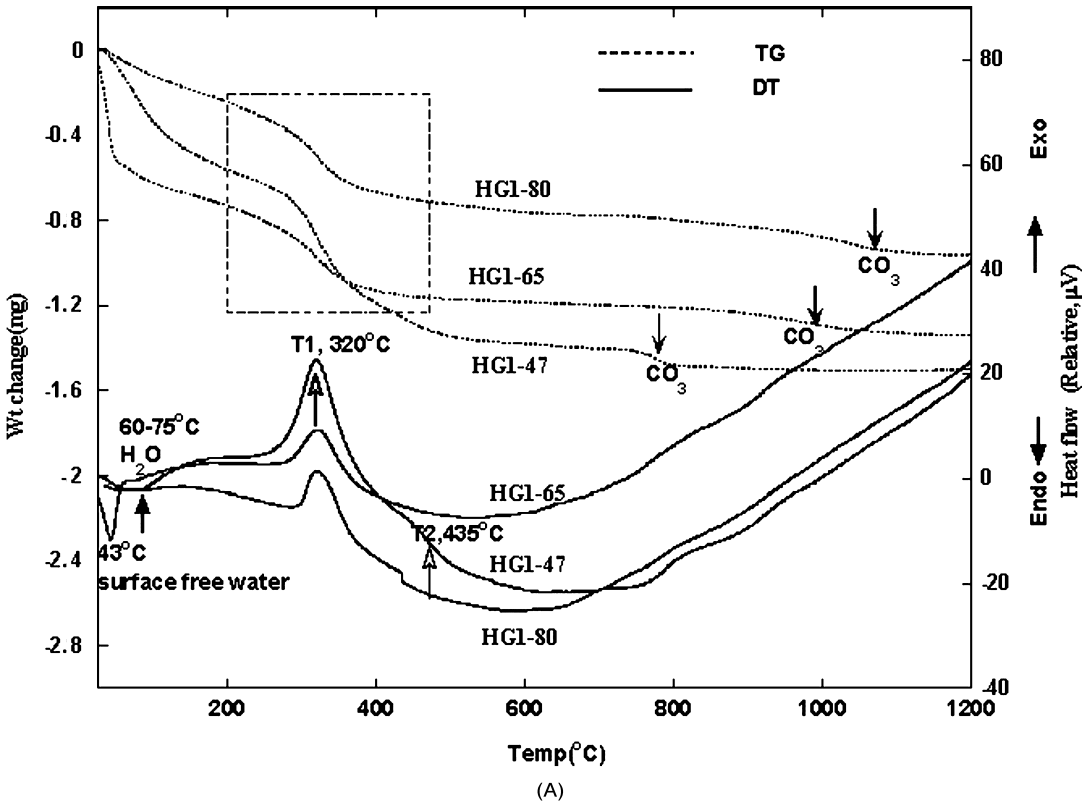

Fig. 2 DT/TG analysis for HG1-47, HG1-65 and HG1-80 samples. HG65 has two endothermic peaks; the first one at 43°C is very strong due to the free surface water and the second one at ∼60°C is weak due to the loosely bound water on HAp structure. Actually most of water in HG65 is the surface water left during the drying process in incubator at 37°C. The loosely bound water peaks for HG1-85 and HG1-47 are appeared at 60 and 75°C, respectively. If we remove the effect of surface water in HG1-65 the organic content of HG1-65 is close to that of HG1-80.

Phosphate band

There are four vibrational modes theoretically present for phosphate ions: $\nu 1$, $\nu 2$, $\nu 3$, and $\nu 4$. As shown in Fig. 3B the $\nu 1$ and $\nu 3$ phosphate modes appear in the region 1200–900 cm^{-1} and another two bands of $\nu 2$ and $\nu 4$ modes appear in the region 700–450 cm^{-1}. The high PO_4 bands (1200–900 cm^{-1}) and the low PO_4 bands (700–450 cm^{-1}) indicate the existence of HAp phase. HG1-65 and HG1-80 show the very strong PO_4 band spectra, indicating the higher content of HAp phase in the composite, but the PO_4 band spectra of HG1-47 is indicating the relatively lower content of HAp in the composite. Normally in HAp/GEL nanocomposite samples the phosphate $\nu 1$ band is centered at the unique position of 962 $cm^{-1}$with narrow band spectra, indicating little change in the P-O stretching energy with the reaction temperature. On the other hands the phosphate $\nu 3$ domain in the range 1200–980 cm^{-1} is well influenced by the quality of apatitic phases in GEL, and so the number of deconvolution components using GRAMS AI was normally above 10, indicating the complicate band structure [22]. The spectra feature of phosphate $\nu 3$ domain is a good guide for understanding the organic-inorganic interaction and the crystal formation of calcium phosphate phase. The phosphate $\nu 3$ band at 1031 cm^{-1} is assigned to the P-O stretching in symmetry PO_4 mode of HAp crystal and there are several other modes such as an asymmetry PO_4 mode at 1097 cm^{-1}, a poor crystalline PO_4 mode at 1015 cm^{-1} and a labile nonapatitic PO_4 mode at 1141 cm^{-1}. From 1141 cm^{-1}band we can think that the nonapatic phase is reduced with the increase of reaction temperature. This is reasonable from the comparison of XRD diffraction patterns in Fig. 1.

Hydroxyl band

Normally the band spectra between 3200 cm^{-1} and 3800 cm^{-1} are highly influenced by the O-H stretching (Fig. 3A). As HAp related bands (Fig. 3B, C) there are OH stretching(3572 cm^{-1}) and liberational bands(632 cm^{-1}) [23]. The OH stretching band at 3572 cm^{-1}belongs to the OH group along the c-column of HAp lattice. In HG1-65 and HG1-80 it is noted that the intensity of OH stretching band (3572 cm^{-1}) is much stronger than that of pure HAp (HAP-37). There is a peculiar new peak centered at 3648cm^{-1} for HG1-65 and HG1-80, which is not normally appeared in other low temperature samples. There is a typical H-O-H band centered at

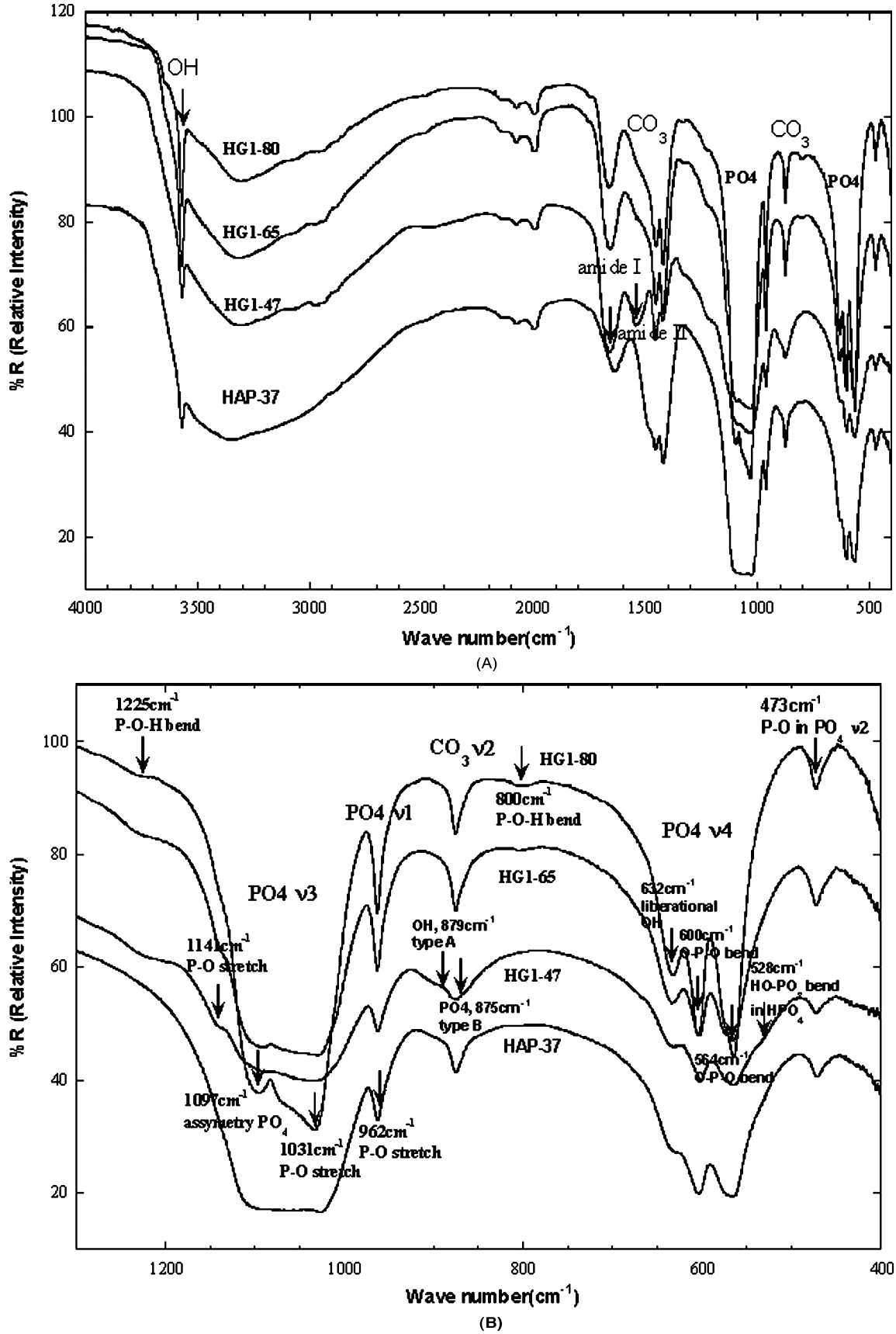

Fig. 3 (A) Wide scanned FT-IR spectra for HAP-37, HG1-47, HG1-65 and HG1-80. The organic coordination of HAp with GEL matrix is confirmed from amide I, II bands and PO_4 bands with the reaction temperature. Narrow scan spectra for PO_4 bands (B), OH bands (C) and CO_3 bands (D), respectively.

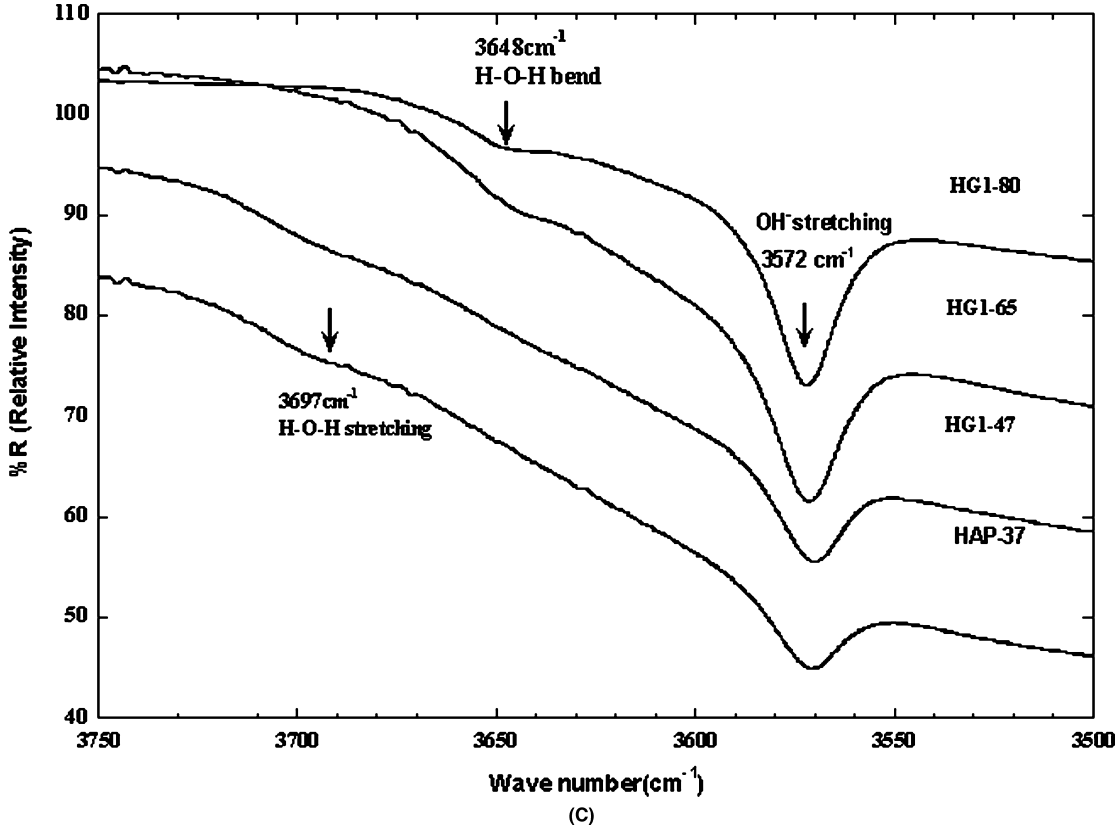
3648cm-1
H-O-H bend
HG1-80
OH- stretching
3572 cm-1
HG1-65
3697cm-1
H-O-H stretching
HG1-47
HAP-37
% R (Relative Intensity)
Wave number(cm-1)
(C)

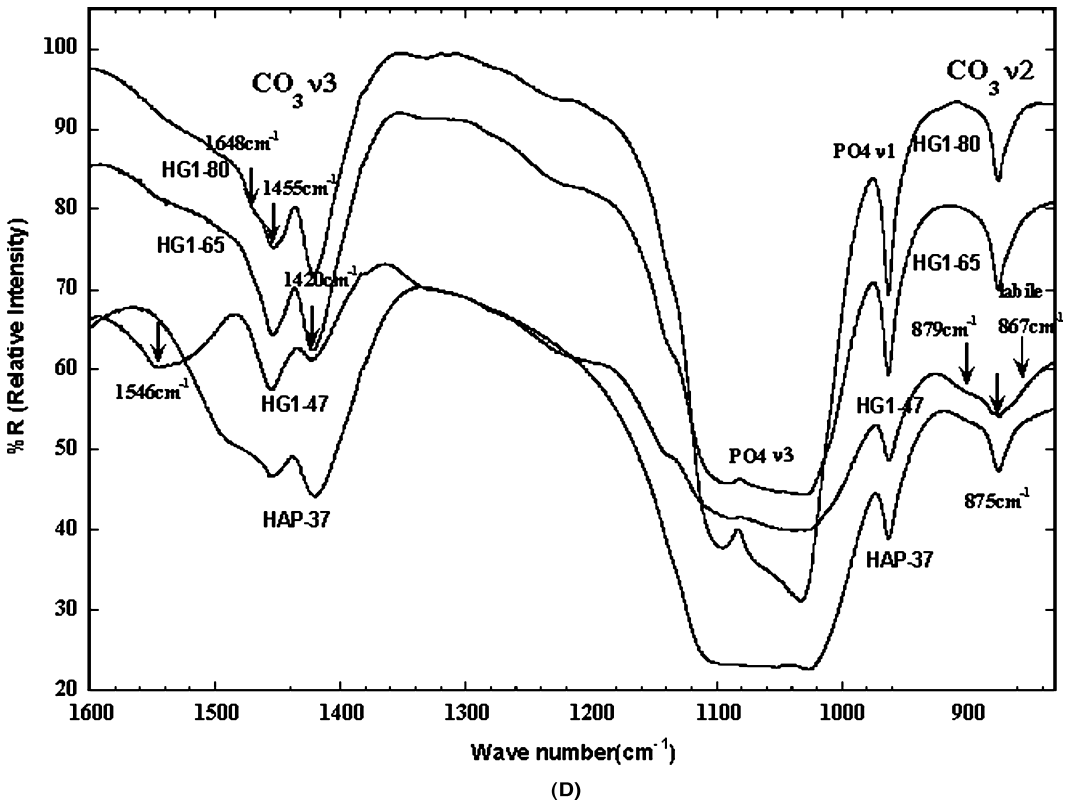
CO3 ν3
CO3 ν2
1648cm-1
HG1-80
1455cm-1
PO4 ν1
HG1-80
HG1-65
1420cm-1
HG1-65
labile
879cm-1
867cm-1
1546cm-1
HG1-47
HG1-47
PO4 ν3
875cm-1
HAP-37
HAP-37
% R (Relative Intensity)
Wave number(cm-1)
(D)

Fig. 3 *Cont.*

3697cm^{-1} in HAp and HG1-47, respectively. The 3648 cm^{-1} band also will be arising from the H-O-H vibration, caused by the binding energy of water molecules on HAp surface. It seems that the binding energy of water molecules on HAp surface (HG1-65, HG1-80) is considerably influenced by the organic interface structure. The organic coordination of H_2O molecules on HAp surface may cause the perturbed H-O-H band at 3648cm^{-1}. It is noted that OH^- band is a little bit shifted from 3570 cm^{-1} (HAP-37, HG1-47) and 3572 cm^{-1}(HG1-65, HG1-80). Therefore it is considered that the organic interface structure of HAp crystal in high temperature sample is much different from those of the low temperature sample.

Carbonate band

Theoretically, carbonate ions have four vibrational modes, three of which are observed in the infrared spectrum and two of which are observed in the Raman spectrum [24]. Normally $\nu 2$ and $\nu 3$ vibrational modes are of importance for IR investigations. The $\nu 1$ mode is masked by the PO_4 $\nu 3$ band and $\nu 4$ mode is very weakly appeared. Peaks in the region 1500–1400 cm^{-1} are due to $\nu 3$ vibrational mode of carbonate ions, and peaks in the region 900–830 cm^{-1} are due to the CO_3 $\nu 2$ vibrational mode. Peaks for $CO_3 \nu 4$ vibrational mode are appeared in the range 780 – 650 cm^{-1} and in our samples two weak $\nu 4$ bands [25] could be identified at 748 and 667 cm^{-1}through the narrow scan and the second derivatives analysis (GRAMS AI). The CO_3 $\nu 3$ band (Fig. 3D) has undergone peak-splitting into two peaks centered at 1420 and 1455 cm^{-1}, and the distribution of the carbonate $\nu 3$ sites depends on the maturation and formation of apatite crystals. Occupancy of the $\nu 2$ sites is considered to occur competitively between the OH^- and carbonate groups at the interface of the growing crystal, whereas occupancy of the $\nu 3$ sites depends on the competition between the phosphate and carbonate ions [26, 27]. From bands analysis [GRAMS AI] (Fig. 3D) all samples mostly belong to type B (CO_3 for PO_4) and at least we can say that CO_3 substitution in HG1-47 is closer to type-B than that of HG1-65 or HG1-80. In HG1-80 we can confirm the weaker peak at 1468 cm^{-1} (type A) with two strong peaks (type B) at 1455 cm^{-1} and 1420 cm^{-1}, indicating the relatively small amount of type-A substitution. Normally type A carbonate apatite is obtained by solid-state reactions at 1000 °C and type B carbonate apatite is prepared at 25–100 °C in aqueous solution [21].

3.3.2. Interfacial bond between HAp and GEL

From the O-P-O bending modes (PO_4 ν_4) and P-O stretching modes (PO_4 $\nu_{1,}\nu_{2,}\nu_3$) as shown in Fig. 3B it is considered that HG1-65 and HG1-80 belong to the same kind of spectra feature, compared with those of HG47. The PO_4 ν_3 domain is an indicator of the amount of HAp in the sample, but the PO_4 $\nu_1$and ν_2 bands reflect the effect of the higher crystallization of HAp. There are two kinds of P-O-H bending mode at 800 and 1225 cm^{-1}, respectively. The 1225cm^{-1} mode reflects the organic coordination of HAp phase with GEL and the 800 cm^{-1} mode is specific only for higher temperature sample of HG1-65 and HG1-80. The modes of P-O stretching (PO_4 ν_1, ν_2) and P-O-H bending at 800cm^{-1} are critically influenced by the organic-inorganic interaction with the reaction temperature or the resultant crystallinity. It is believed that P-O stretching modes in $PO_4\nu_3$domain also show the same kind of tendency with the temperature in spite of the complicate band feature.

From P-O-H bending modes (1225 and 800cm^{-1}) the 1225cm^{-1} band represents the same kind of organic coordination with the reaction temperature. On the other hands the 800 cm^{-1} band shows a different kind of organic coordination between high temperature sample (HG1-65, HG1-80) and low temperature one (HG1-47). That is, the 800cm^{-1} band reveals the P-O-H stretching motion caused by the different interfacial structure between HAp and the critically degraded GEL. When the reaction is occurred above 50°C during the coprecipitation the GEL molecules are quickly degraded. However, the composite particles of HAp and GEL, which once coordinated, can exist stably even during the high temperature aging. It seems that HAp/GEL nanocomposite slurries, once formed, have the structural stability and keep the organic-inorganic interface. During the coprecipitation process each of GEL molecules will experience the different degradation with the reaction temperature and the mixing kinetics. So the interfacial structure of the resultantly formed composite can be locally different.

3.4. TEM and ED pattern

From Fig. 4 we can observe needle-shaped particles and the HAp crystals in HG1-65 (12nm × 150nm) are nearly twice thicker than HG1-47 (7nm × 100nm). In HG1-80 HAp phase was grown to the bigger crystals of (150 – 300) nm × (800 – 2000) nm size and the crystals were a single crystal grade from ED pattern. HG1-47 showed the clear diffraction ring patterns comprised of (002) and (112) spots with a weak inner ring of (210) diffraction, indicating the coagulation of very tiny HAp crystals. In HG1-65 the diffraction spots of (002) and (112) ring patterns were getting stronger, indicating the stronger development of HAp crystals with the clear (210) diffraction. In HG5-37 (Fig. 4D) the crystals are 4–5 nm thick and it is judged that HAp nanocrystals are preferentially aligned along the c-axis, from the direction

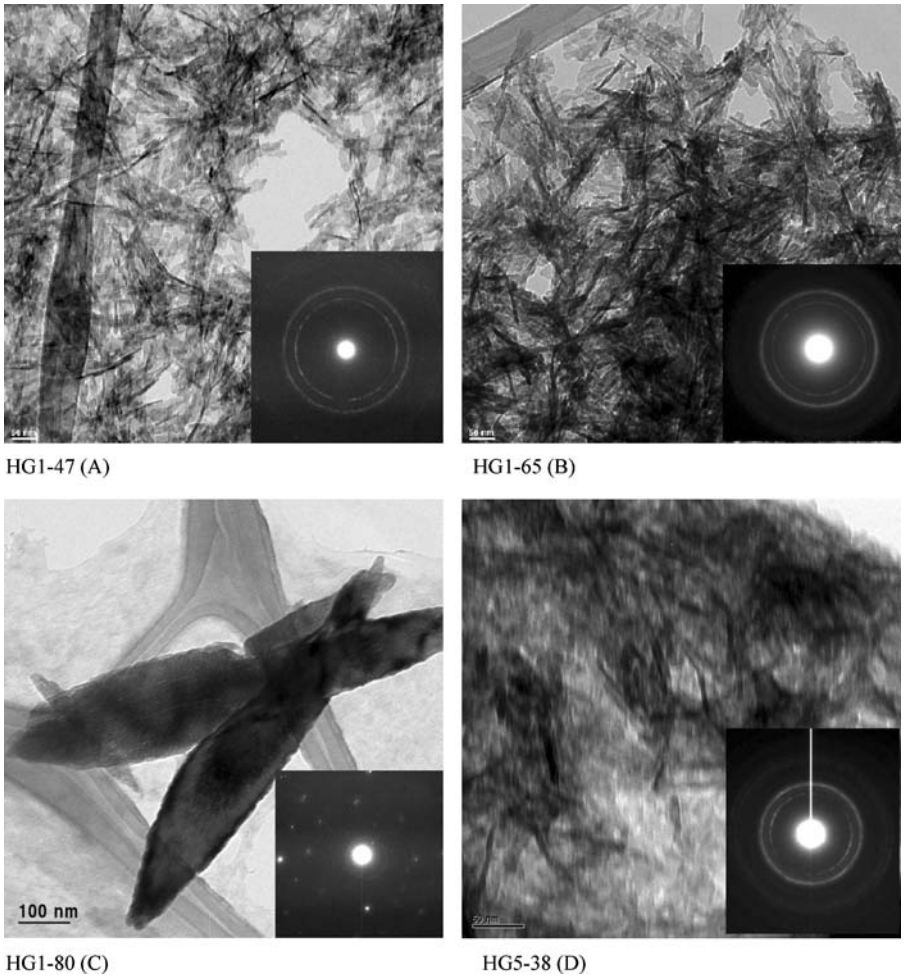

Fig. 4 TEM morphology and ED pattern for the samples synthesized at 47 °C (A), 65 °C (B), 80 °C (C). (D) is for HG5-37 sample, which was prepared at 37 °C for GEL 5g batch. ED pattern for HG5-37 shows the preferred orientation of HAp crystals along c-axis of GEL molecule. The scale bars are 50nm for (A), (B) and (D), and 100 nm for (C), respectively.

of the arc-like (002) diffraction spots. In the HG1-47 sample the (002) spots are centered on the ring, meaning the random distribution of HAp crystals. Normally the molecular structure of type-I COL is denatured above 40 °C and the commercial GEL partially keeps its self-assembling activity in spite of the denaturation during the production process. When the coprecipitation is occurred at 37 °C the HAp/GEL composite shows the preferred orientation of c-axis in HAp crystal development. However, the HAp/GEL composite prepared at 47 °C doesn't show the preferred orientation of c-axis of HAp crystals because of the deprival of the self-assembling activity. Normally GEL has the partial activity for self-assembling and the activity is mostly disappeared above ∼40 °C, but the organic-inorganic interaction is still working up to higher temperature above 80 °C. Below 50 °C HAp phase is heterogeneously nucleated and gently growing on the GEL molecules matrices as shown in Fig. 4(A) and (D). Above 50 °C the growth of HAp crystal becomes dynamic and the pattern of crystal growth is close to the hydrothermal behavior as shown in Fig. 4(B) and (C).

3.5. SEM micrograph

When a liquid droplet of GEL with H_3PO_4 meets the free Ca^{2+} ions released from the hydrated $Ca(OH)_2$ suspension, lots of calcium phosphate nano-crystals are formed and dispersed into the GEL liquid drop. HAp/GEL composite slurries can be grown through the interconnection with another slurries during aging process. After aging the slurries are collected as a cake through the vacuum filtering. Fig. 5B(HG1-65) and 5C(HG1-80) well show the coagulated pattern of HAp crystals in GEL matrices after drying at room temperature. Essentially this-like coagulation pattern will be same in HG1-47(Fig. 5A) and HG4-37(Fig. 5D), but lots of tiny crystals are embedded in plenty of organics. Under higher magnification HG1-47 and HG4-37 show a distinct aggregate having lots of tiny crystals and this aggregate is appeared like a grain($\sim 2\mu$m size) in Fig. 5A and 5D.

From SEM morphology HG1-65 (Fig. 5B) shows a rough coagulation of needle particles and HG1-80 (Fig. 5C) shows a coagulation of more strongly developed needle particles. HG1-47 (Fig. 5A) shows a dense body having 3 point bending

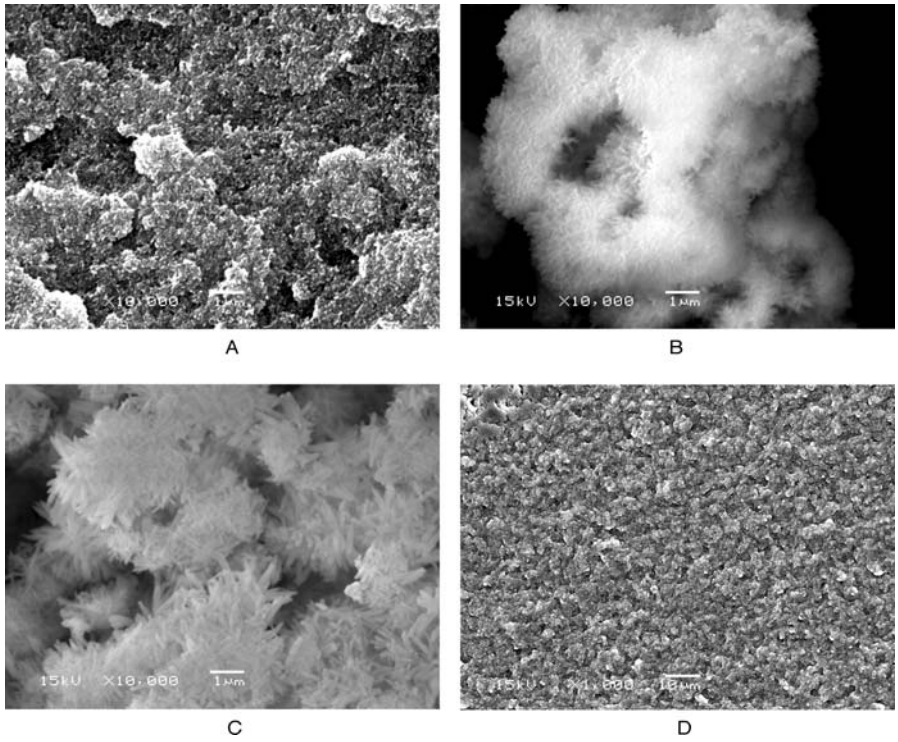

Fig. 5 SEM morphology for HG1-47(A), HG1-65(B), HG1-80(C) and HG4-37(D). The sample HG4-37(D), prepared at 37 °C shows a very dense microstructure. HG1-65 and HG1-80 samples show the coagulation of needle particles. The scale bars are 1μm for (A), (B) and (C), and 10 μm for (D), respectively.

strength of 20 Mpa, and HG4-37 sample(Fig. 5D) is denser and has higher bending strength above 30 Mpa. A dense body was obtained if the sample is prepared below 50 °C, but a porous body was obtained if the sample is prepared above 50 °C.

3.6. Organic-inorganic interaction

Generally the crystal growth in aqueous solution is based on the diffusion process, that is, thermally activated process. In HG1-47, HG1-65 and HG1-80 samples the temperature only was changed for the constant amount of GEL, Ca^{2+} and PO_4^{3-} in a batch. So it can be considered that the number of functional groups of GEL coordinated with Ca^{2+} ions of HAp is constant. If the functional groups in GEL persistently exist during the entire coprecipitation and aging, the formation and growing of HAp crystals nuclei will be thermodynamically controlled on the GEL molecules.

The GEL aqueous solution was mixed with H_3PO_4 and kept for 12 hrs before the coprecipitation process, because the pretreated mixture solution of GEL and H_3PO_4contributed to the uniformity and the reactivity of GEL solution. The commercial GEL precursor has variety of fibril structures because of the denaturation process during the production. So the pretreatment with H_3PO_4 helps the uniformity of the GEL molecular structure through further disintegration. Until now the quantitative criterion for the pretreatment schedule of GEL in H_3PO_4 solution was not definitely defined, but too long treatment above one day was very harmful to produce the well organized HAp crystals after the coprecipitation. At this point we consider that GEL molecules were well activated and in some parts further denatured through the aging with H_3PO_4. Below 50 °C the degradation of GEL molecule structure was gently occurred, but above 50 °C the GEL molecules were more strongly degraded. Above 50 °C the number of eligible nucleation sites for HAp crystals was greatly limited and so the bigger crystals were induced. From these discussions we can say that the organic-inorganic interaction prevails below 50 °C and the HAp crystal development prevails above 50 °C. That is, below 50 °C the HAp crystal developing reaction is suppressed by the prevailing organic-inorganic interaction.

4. Conclusion

From the HAp crystal development in GEL matrix with the temperature there was a competition between organic-inorganic interaction and thermodynamic reaction for HAp crystal growing. The transition in these two mechanisms was occurred at ∼50 °C and the reason is attributed to the critical change of the degraded structure of GEL molecule at this temperature. So the reaction temperature should be chosen below 50 °C in order to develop the optimum preparation condition for obtaining the tough HAp /GEL composite materials.

Acknowledgements The author, M. C. Chang, greatly thanks Dr. Edward Rustamzadeh for his surgical leadership. The revision work of this paper was possible by virtue of him with his brain surgery team in Hennepin County Medical Center.

References

1. R. A. YOUNG, *Clinical Orthopedics* **113** (1975) 249.
2. C. F. NAWROT and D. J. CAMPBELL, *J. Dent. Res.* **56** (1977) 1017.
3. S. MANN and G. A. OZIN, *Nature* **365** (1996) 499.
4. S. MANN, D. D. ARCHIBALD, J. M. DIDYMUS, T. DOUGLAS, B. R. HEYWOOD, F. C. MELDUM and J. R. NICHOLAS, *ibid* **382** (1993) 313.
5. M. MUTHUKUMAR, C. K. OBER and E. L. THOMAS, *Science* **277** (1997) 1225.
6. S. I. STUPP and P. V. BRAUN, *ibid* **277** (1997) 1242.
7. A. L. BOSKEY, *Cacif. Tissue Int.* **63** (1998) 179.
8. F. PETERS and M. EPPLE, *J. Chem. Soc. Dalton Trans.* (**24**) (2001) 3585.
9. M. IIJIMA, in "Monogr. Oral. Sci. Vol. 15, Octacalcium phosphate; Formation of octacalcium phosphate *in vitro*." (Kager, Basel, 2001) p. 17–49.
10. S. BUSCH, H. DOLHAINE, A. DUCHESNE, S. HEINZ, O. HOCHREIN, F. LAERI, O. PODEBRAD, U. FIETZ, T. WEILAND and R. KNIEP, *Eur. J. Inorg. Chem.* **10** (1999) 1643.
11. S. BUSCH, U. SCHWARTZ and R. KNIEP, *Advanced Functional Materials* **12** (203) 189.
12. M. KIKUCHI, Y. SUETSUGU, J. TANAKA, S. ITO, S. ICHINOSE, K. SHINOYAMA, Y. HIRAOKA, Y. MANDAI and S. NAKATANI, *Bioceramics* **12** (1999) 393.
13. M. C. CHANG, T. IKOMA, M. KIKUCHI and J. TANAKA, *J. Mat. Sci. Lett.* **20** (2001) 1129.
14. M. C. CHANG, T. IKOMA, M. KIKUCHI and J. TANAKA, *J. Mat. Sci. Mat. Med.* **13** (2002) 993.
15. M. C. CHANG and J. TANAKA, *Biomaterials* **23** (2002) 3879.
16. M. C. CHANG and J. TANAKA, *ibid.* **23** (2002) 4811.
17. M. C. CHANG, C.-C. KO and W. H. DOUGLAS, *ibid.* **24** (2002) 2853.
18. M. C. CHANG, C.-C. KO and W. H. DOUGLAS, *ibid.* **24** (2002) 3087.
19. A. G. WORD and A. COURTS, in "The science and technology of gelatin" (Academic Press, London; 1977).
20. A. VEIS, in "The macromolecular chemistry of gelatin" (Academic Press, London; 1964).
21. R. Z. LEGEROS, in "Monogr. Oral. Sci. Vol. 15, Calcium Phosphates in Oral Biology and Medicine" (Kager, Basel, 1998) P.1.
22. E. P. PASCHALIS, E. DICARLO, E. BETTS, P. SHERMAN, R. MENDELSOHN and A. L. BOSKEY, *Calcif. Tissue Int.* **59** (1996) 480.
23. R. Z. LEGEROS, G. BONEL and R. LEGEROS, *Calcif. Tiss. Res.* **26** (1978) 111.
24. D. G. A. NELSON and J. D. B. FEATHERSTONE, *Calcif. Tissue Int.* **34** (1982) 569.
25. H. E. FEKI, C. REY and M. VIGNOLES, *ibid.* **49** (1991) 269.
26. M. A. WALTERS, Y. C. LEUNG, N. C. BLMENTHAL, R.Z. LEGEROS and K.A. KONSKER, *J. Inorgan. Biochem.* **39** (1990) 193.
27. J. C. ELLIOTT, D. W. HOLCOMB and R. A. YOUNG, *Calcif. Tissue Int.* **37** (1985) 372.